

## Retraction

# Retracted: Comprehensive Evaluation of Shale Reservoir Reconstruction based on Microseismic and Multidisciplinary Integration

### Adsorption Science and Technology

Received 20 June 2023; Accepted 20 June 2023; Published 21 June 2023

Copyright © 2023 Adsorption Science and Technology. This is an open access article distributed under the Creative Commons Attribution License, which permits unrestricted use, distribution, and reproduction in any medium, provided the original work is properly cited.

This article has been retracted by Hindawi following an investigation undertaken by the publisher [1]. This investigation has uncovered evidence of one or more of the following indicators of systematic manipulation of the publication process:

- (1) Discrepancies in scope
- (2) Discrepancies in the description of the research reported
- (3) Discrepancies between the availability of data and the research described
- (4) Inappropriate citations
- (5) Incoherent, meaningless and/or irrelevant content included in the article
- (6) Peer-review manipulation

The presence of these indicators undermines our confidence in the integrity of the article's content and we cannot, therefore, vouch for its reliability. Please note that this notice is intended solely to alert readers that the content of this article is unreliable. We have not investigated whether authors were aware of or involved in the systematic manipulation of the publication process.

Wiley and Hindawi regrets that the usual quality checks did not identify these issues before publication and have since put additional measures in place to safeguard research integrity.

We wish to credit our own Research Integrity and Research Publishing teams and anonymous and named external researchers and research integrity experts for contributing to this investigation.

The corresponding author, as the representative of all authors, has been given the opportunity to register their agreement or disagreement to this retraction. We have kept a record of any response received.

### References

- [1] H. Chen, D. Fang, H. Gu, and W. Huang, "Comprehensive Evaluation of Shale Reservoir Reconstruction based on Microseismic and Multidisciplinary Integration," *Adsorption Science & Technology*, vol. 2022, Article ID 5095254, 18 pages, 2022.



## Research Article

# Comprehensive Evaluation of Shale Reservoir Reconstruction based on Microseismic and Multidisciplinary Integration

Haidong Chen <sup>1</sup>, Dawei Fang <sup>2</sup>, Hongtao Gu,<sup>3</sup> and Wenzhuo Huang<sup>4</sup>

<sup>1</sup>Schlumberger, Beijing 100016, China

<sup>2</sup>Anhui University, Hefei Anhui 230039, China

<sup>3</sup>Sinopec Chongqing Shale Gas Co., Ltd, R&D Experimental Center, Chongqing 408499, China

<sup>4</sup>Weatherford, Chengdu Sichuan 610599, China

Correspondence should be addressed to Dawei Fang; 19207191@masu.edu.cn

Received 25 July 2022; Revised 12 August 2022; Accepted 13 August 2022; Published 22 September 2022

Academic Editor: Rabia Rehman

Copyright © 2022 Haidong Chen et al. This is an open access article distributed under the Creative Commons Attribution License, which permits unrestricted use, distribution, and reproduction in any medium, provided the original work is properly cited.

Microseismic can build a bridge between engineering operations such as drilling and fracturing and stratum evaluation such as earthquake, geology, and logging by fully excavating fracture time, spatial development characteristics, and focal information. For the postseismic evaluation of microseisms, a comprehensive evaluation system integrating microseisms and multidisciplines is established in this paper; through deep excavation of microseismic information such as the time and space distribution of microseismic events, quantitative statistics, magnitude-frequency gradient ( $B$ -value) and S-P wave energy ratio ( $E_s/E_p$ ), the effective identification of dry faults, wet faults, cracks, joints, sweet spots and nonsweet spots is realized, combined with seismology and geology. The engineering problems (casing change, pressure change, fracturing barrier, etc.) are analyzed accordingly, which enhances the comprehensive evaluation function of microseismic and multidiscipline.

## 1. Introduction

Shale gas is an important field of unconventional natural gas exploration and development [1]. It mainly exists in the micro-nano pores of shale and exists in two forms: free state and adsorption state. China is rich in shale gas resources, mainly distributed in the south, mainly in Paleozoic marine shale formations, especially in Silurian Longmaxi Formation and Cambrian Qiongzhusi Formation [2, 3]. Compared with conventional oil and gas reservoirs, shale gas reservoirs have the characteristics of self-generation, self-storage, low abundance, continuous distribution, low porosity, and low permeability, and it is difficult to form natural productivity [4]. Therefore, shale gas development must adopt a series of stimulation measures, such as fracturing to release shale gas and obtain economic benefits [5–7]. The core technology of shale oil and gas resources development is horizontal well and hydraulic fracturing technology. It is particularly important to identify the distribution and development of hydraulic fracturing fractures by means of microseismic

monitoring. However, in actual production, the application of microseismic technology is not perfect, and the identification of fracturing fractures and the evaluation of reservoir after fracturing by using various information obtained by microseismic has always been a problem that needs to be studied.

To improve the efficiency of shale gas exploration and development, it is necessary to strictly control the single well investment and reduce the cost [8]. The traditional interpretation of reflected seismic data is mainly based on the propagation law and geological characteristics of seismic waves, transforming various seismic wave information into information such as structure and formation lithology, and transforming seismic profiles into geological profiles for interpretation. For the exploration and development of unconventional oil and gas, it is necessary to carry out fracture interpretation and evaluation after reservoir fracturing. The microseismic monitoring data during fracturing provides reservoir evaluation information different from the reflection seismic data. Microseismic monitoring can ensure



the best effect of hydraulic fracturing as much as possible on the premise of ensuring construction safety and controlling fracturing cost through real-time monitoring. It is an indispensable factor of shale gas revolution in the United States that microseismic monitoring can obtain the time and space distribution information of fractures and provide effective technical support for fracturing reconstruction by combining various information related to engineering and geology.

Microseismic is a weak seismic wave, i.e., weak seismic signal, produced by rock fracture caused by stress field change in rock mass. Microseismic is different from artificial earthquake in seismic exploration. It occurs naturally in the production process and has the characteristics of small energy and short duration. The acoustic emission phenomenon caused by the fracture of underground rock mass is called microseismic event. Microseismic monitoring technology is the most accurate, timely, and informative monitoring method for hydraulic fracturing fractures [9]. Its application in hydraulic fracturing mainly includes three aspects: real-time monitoring, comprehensive evaluation of fracturing effect, and development scheme design. The so-called comprehensive evaluation of fracturing effect means that by providing the space-time distribution characteristics of fractures, analyzing the potential geological information and laws of seismic source information according to the amplitude and statistics characteristics of signals, and relying on the development characteristics of artificial fractures and natural fractures, it can be integrated with previous earthquake, geology, and logging research and engineering-related information such as drilling, cementing, and fracturing, so as to achieve the purpose of comprehensive evaluation. With the continuous evolution of production needs and the in-depth research on shale gas, unconventional oil and gas exploitation and various new energy exploitation, microseismic monitoring technology, as the core of its dependence, has become an important guarantee for ensuring efficiency and personnel and equipment safety. It is mostly used as a judgment basis for judging the formation and development trend of fracturing fractures.

## 2. Microseismic Source Information

The joint inversion of microseismic and ground observation data also improves the accuracy of source location, which directly affects the interpretation of reservoir fracture. At present, in the practical application of microseismic inversion, the source location data is widely used, but the application of the source mechanism and the seismological data related to the source mechanism is not sufficient. In fact, the focal mechanism of microseismic is directly related to the characteristics of reservoir media, the occurrence of fracture development, and the direction of formation stress. It is very important to evaluate and interpret the fracturing effect by using the seismological parameters obtained from microseismic inversion.

A large number of microseismic event points are obtained by microseismic positioning, and these event points contain a large amount of source information, mainly including source type information, time information, loca-

tion information (x, y, and z coordinates), precision parameters, source-related parameters, source mechanism-related parameters, and quality control-related parameters (Table 1). Through the comprehensive application of these information, the real-time monitoring of hydraulic fracturing and comprehensive evaluation after fracturing can be achieved.

Part of the seismic source information is directly acquired during the acquisition and processing, such as number, type, date and time, number of picked-up P-wave and S-wave, spatial position (x, y, and z coordinates), P-wave energy, S-wave energy, P-wave velocity ratio, signal-to-noise ratio, and root-mean-square noise. Others need to be obtained by indirect means, such as focal radius, positioning error, polarization error, seismic moment, moment magnitude, main frequency, moment tensor parameters, and T-k diagram. The related energy parameters are mainly reflected by the energy after electromechanical conversion. Based on the energy of P-wave and S-wave, the seismic moment, moment magnitude, and other parameters are obtained.

The two most important results obtained from microseismic monitoring are the spatial location and focal parameters of microseismic events, according to which the fracture process and development characteristics can be described. The spatial distribution of microseismic events can provide the spatial location of fractures. The microseismic events of each fracturing section may occur in the adjacent sections, which indicates that the primary fractures of the adjacent unfractured sections may be activated during the fracturing reconstruction of the reservoir, so that the microseismic events occur in the adjacent fracturing sections. Therefore, the changes of the fracturing fractures can be qualitatively analyzed according to the spatial-temporal distribution of the microseismic events. After the spatial position of microseismic events is determined, the difference between the time difference of P-wave and S-wave obtained by forward modeling of each geophone and the time difference actually picked up is the time error. The error between the azimuth obtained by polarization analysis of each geophone and the spatial position of microseismic events and the azimuth of the geophone is azimuth error, and a residual error is obtained by averaging them, respectively.

The most commonly used source parameter is source intensity, which is generally expressed by magnitude, which is a measure of energy. The place where the vibration is caused by the rupture of the rock layer in the earth is called the focal point. It is an area with a certain size, also known as the focal area or focal body, and it is the place where seismic energy is accumulated and released. Using seismic waveform data for seismic moment tensor inversion, people can roughly distinguish the characteristics of these two sources. There are four commonly used magnitude scales: local magnitude ML, surface wave magnitude MS, body wave magnitude Mb, and moment magnitude MW [10]. There are also a series of problems about the magnitude: first, these are all obtained by experience, and there is no physical model associated with them, so it is impossible to accurately give the relevant information of the fault when the magnitude is given. Another more practical problem is that these



TABLE 1: Information table of microseismic events.

Type	Description
Types of microseismic signals	Number and type (such as perforation signal, microseismic signal, seismic wave, and noise)
Time	Year, month, day, hour, minute, second, millisecond
Positional information	North (X), east (Y), depth (Z)
Accuracy parameter	Positioning error, residual error, polarization error
Seismic source correlation parameter	Seismic moment, moment magnitude, P-wave energy, S-wave energy, S-wave energy ratio ( $E_s/E_p$ ), focal radius, and S-wave dominant frequency
Focal mechanism-related parameters	Tensor parameters (such as double couple component DC, compensated linear vector coupling CLVD, and isotropic volume component ISO), T-k diagram
Quality control-related parameters	Signal-to-noise ratio, root-mean-square noise (RMS error), number of picked-up P-wave and S-wave

magnitudes are aimed at the largest earthquakes. The concept of moment [11] overcomes these shortcomings, and the formula is

$$M_w = \frac{2}{3} (\lg M_0 - 9.1). \quad (1)$$

When the seismic moment  $M_0$  is obtained, the moment magnitude  $M_w$  [12–14] can be calculated. Moment magnitude can reflect the magnitude of slip on the fracture surface, and it is deduced by waveform inversion [15, 16]. Moment magnitude is established by empirical and theoretical modeling research in seismology [17]. Seismic moment  $M_0$  can measure the energy generated by stratum rupture and sliding and is the couple moment of one of the equivalent couples of the source. Its expression is

$$M_0 = \mu D A. \quad (2)$$

The unit is N.m (nm), where  $\mu$  is the stiffness coefficient of the medium,  $D$  is the dislocation quantity of the fracture, and  $A$  is the area of the fracture surface. The larger the fracture surface  $A$  is, the longer the period is, and the greater the energy generated.

Focal mechanism-related parameters, namely, moment tensor parameters, are used to identify the volume failure mechanism of an event. They are mainly divided into three components: the dual couple component DC describing shear fracture, the isotropic component ISO (explosion or collapse) describing volume strain, and the compensated linear vector dipole CLVD (describing the strain along one axis, the strain in the other two axes will occur correspondingly, such as crack opening or crack closing). The tensor representation of seismic moment depends on the direction and intensity of the source. The seismic source can be expressed as the sum of expansion source, shear dislocation source, and compensated linear vector dipole by seismic moment tensor.

### 3. Microseismic Signal Analysis

Microseismic monitoring can not only provide magnitude and space-time location information of microseismic events

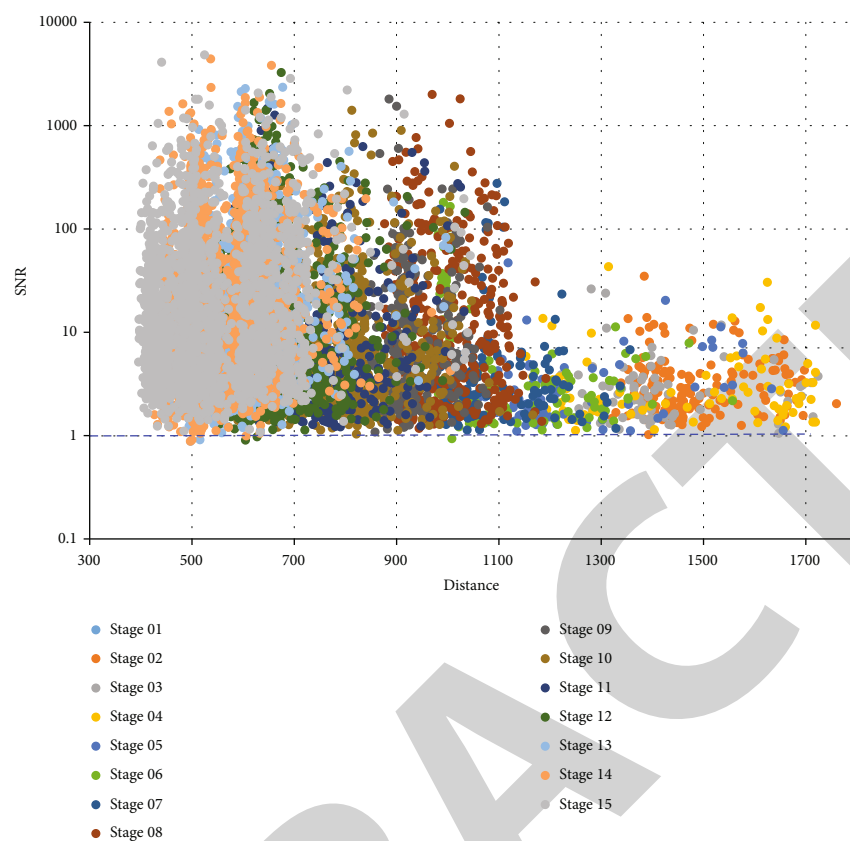
for fracture interpretation, but also its data itself contains a lot of potential information. The microseismic source information is mainly obtained on the basis of ray propagation energy and inversion positioning. Effective and widely used microseismic event analysis methods mainly include statistical analysis of source information, intersection analysis of source information, nodal surface analysis, magnitude-frequency  $b$  value analysis, and moment tensor inversion. By further mining the microseismic information, we can study the fracturing process more fully and obtain the fracture scale, development characteristics, and distribution information of reservoir stress in the fractured area, so as to realize the optimization of reservoir reconstruction.

The magnitudes of most microseismic events are between -2.8 and -2. From the overall distribution of microseismic events, it can be seen that the magnitude in the middle of the fracturing area is relatively small and the distribution is very concentrated, and the magnitude of microseismic events in the fracturing sections on both sides is relatively large and the distribution is relatively scattered. According to the characteristics of strong heterogeneity of the reservoir in the study area, it can be qualitatively explained that the lithological mud content in the middle of the reservoir in the fracturing area is high, the brittleness is poor, and it is not easy to fracture, while the lithological mud content of the reservoirs on both sides is low, the brittleness is good, and it is easy to fracture.

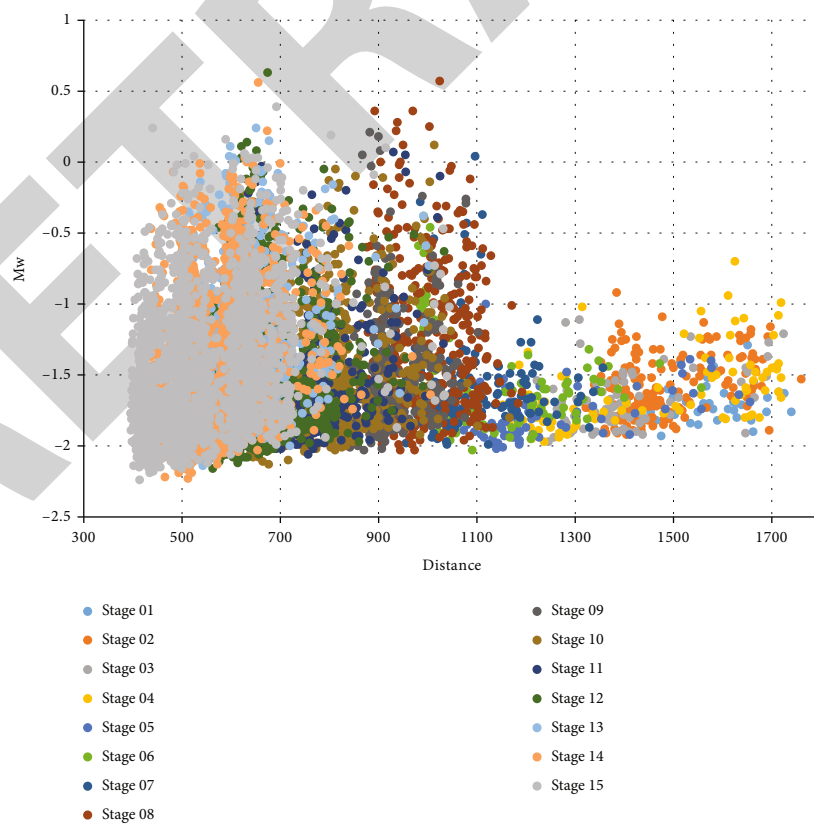
**3.1. Statistical Analysis of Source Information.** Under the condition of homogeneous stratum and the same fracturing scale, the number of microseismic events induced by single-stage fracturing will decrease with the increase of monitoring distance, and the minimum magnitude will increase with the increase of monitoring distance.

Under the condition of heterogeneous stratum, the number, magnitude, and  $E_s/E_p$  of microseismic events received vary with the same fracturing scale and different fracturing areas due to the difference of petrophysical properties of stratum itself. Any condition of distance, matrix, or crack will change the statistical law of the received events. Usually, the microseismic events received in areas with close monitoring distance, good formation brittleness, and developed fractures are characterized by high signal-to-noise ratio,





(a)



(b)

FIGURE 1: Continued.



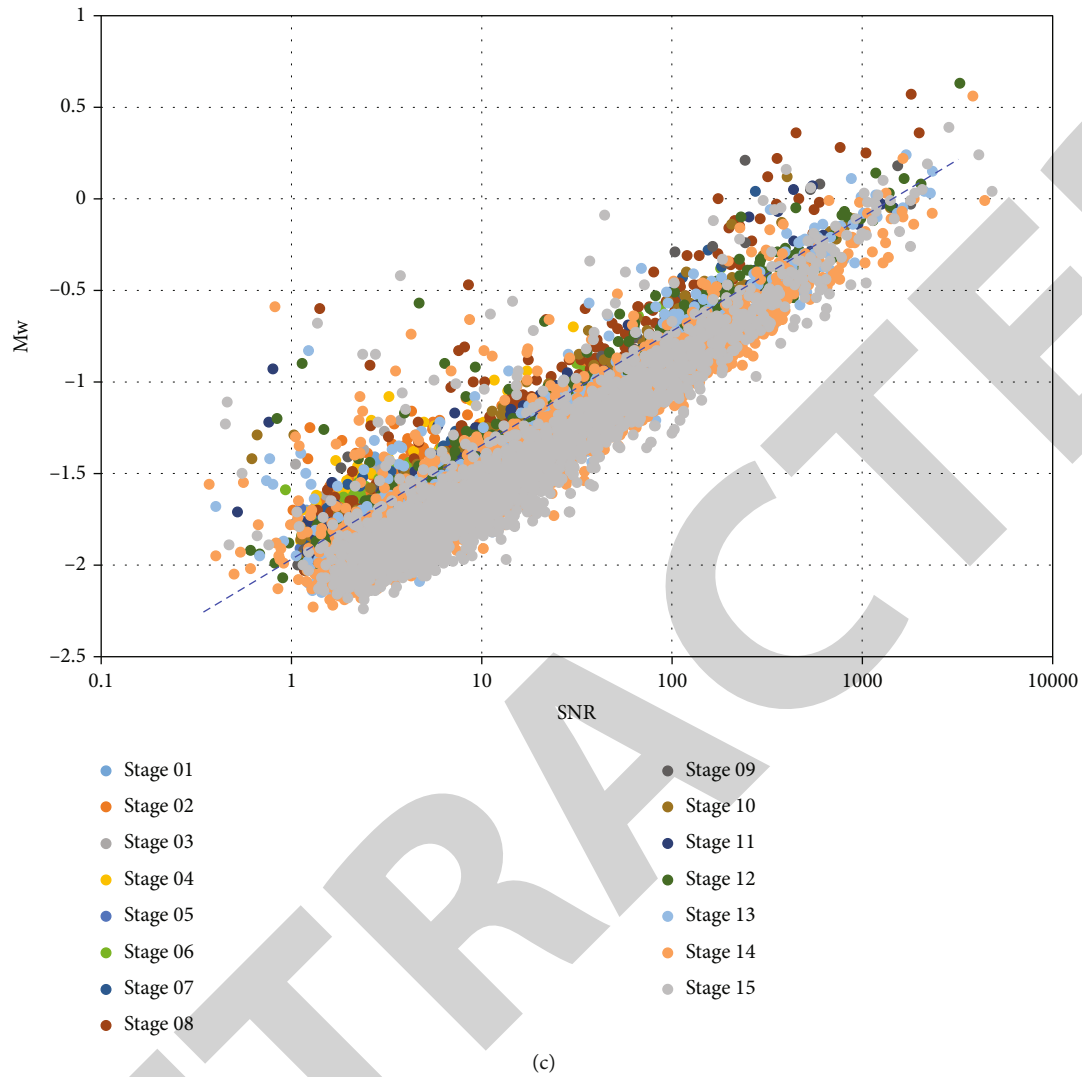


FIGURE 1: Intersection of signal-to-noise ratio SNR and monitoring distance (a), moment magnitude and monitoring distance (b), and moment magnitude and signal-to-noise ratio (c) of microseismic signals.

large number, strong magnitude, and high  $E_s/E_p$  value. By counting the number, magnitude, and  $E_s/E_p$  histograms of microseismic events, the basic evaluation of stratum matrix or fracture can be realized.

**3.2. Analysis of Seismic Source Information Intersection.** Focal intersection analysis is a common method of microseismic interpretation, which is mainly embodied in two aspects: screening of microseismic abnormal events and evaluation of microseismic reliability. Among them, the intersection relationship between magnitude and monitoring distance is the most widely used, through which the reliability of microseismic processing results can be judged. In addition, the intersection relation combined with the magnitude distribution interval can judge the effective monitoring range of microseisms. In addition, the intersection of magnitude and signal-to-noise ratio of microseismic events can be carried out. Through the intersection relationship between magnitude and signal-to-noise ratio, the important role of

signal-to-noise ratio in providing threshold value for microseismic first arrival pickup can be established.

**3.3. Rupture Surface and Nodal Surface.** The rupture surface refers to that when the stress of the rock exceeds its strength, that is, the stress difference exceeds the fracture strength, the fracture begins. At the beginning of the fracture, the microcracks first appear, and the microcracks gradually develop and connect with each other in series to form an obvious fracture surface, that is, the fracture surface where the two walls of the fault slide relative to each other.

The characteristics of microseismic signals are similar to those of natural earthquakes, which are mainly caused by shear dislocation of strata [18, 19]. The microseismic focal mechanism can be solved by using three constraints, namely, the initial polarization of P-wave, the energy ratio of P-wave and P-wave, and the correlation coefficient of waveform [20]. C. Cipolla et al. put forward the radiation pattern diagram of P-wave and S-wave energy and clarified the



relationship between the development direction of faults and P-wave and S-wave energy. It is pointed out that the maximum energy direction of the received P-wave is at an angle of 45 degrees to the direction of the fracture surface, while the maximum energy direction of the received S-wave is parallel or perpendicular to the direction of the fracture surface. The spatial transition of P-wave energy and P-wave energy is very obvious. The low P/SH value means that the azimuth corresponding to the signal received by the geophone is parallel to or vertical to the fracture surface (vertical can be judged according to the distribution law), and the corresponding P-wave energy is very weak, which is called nodal surface. At this position, the energy of P-wave is very weak or nearly disappeared, so it is difficult to locate, and the number of corresponding incident points will be reduced.

**3.4. Evaluation of Magnitude-Frequency Gradient  $b$  Value.** The concept of value was first put forward by Gutenberg and Richter. It mainly adopts the statistical principle and obtains a constant value  $B$  by counting the frequency distribution of rupture events with different moment magnitudes. Main physical significance is as follows: when an earthquake with a strong magnitude occurs, there will be an exponential number of earthquake events with a weak energy level. Its expression is

$$\text{Log}N = A - BM_s, \quad (3)$$

where  $n$  represents the number of events,  $A$  and  $B$  are constants, and gradient  $B$  represents the frequency change of events of different sizes in a series of events. The higher the value of  $b$ , it means that a few high moment magnitude events are accompanied by a large number of small moment magnitude events. The lower  $b$ , the higher moment magnitude events, and the smaller the difference between low moment magnitude events.

$b$  value statistics is an effective way to identify crack types. In practice, interpreters need to select local microseismic event points for statistics according to the spatial distribution characteristics of microseismic events. In order to achieve a stable statistical effect, it is necessary to provide enough incident points. And this statistical analysis is usually only used in fracture analysis after fracturing. Maxwell et al. found that in the process of fracturing, the  $b$  value corresponding to natural fractures or faults is about 1, and the  $b$  value corresponding to artificial fractures is about 2 or higher. It is mainly because in natural fracture development areas, hydraulic fracturing mainly induces microseisms by leakage effect, and fracturing fluid entering faults or natural fractures will produce a large number of high moment magnitude events. If natural fractures are not developed, micro-earthquakes are mainly induced by hydraulic fracturing with tip effect, and high moment magnitude events are few. Therefore, the value of  $b$  is directly related to the nature of fractures, and it can be used to evaluate the natural fractures of hydraulic fracturing under microseismic conditions.

In the field of earthquake prediction, it is found that before a large earthquake, earthquakes within certain magnitude ranges often increase or decrease in the source and

nearby areas, leading to the abnormal phenomenon that the proportion of large and small earthquakes is out of balance and the value of  $b$  decreases. In addition, the increase of regional stress accumulation level is a necessary condition for the occurrence of a large earthquake. Therefore, it is believed that the value of  $b$  reflects the state of in situ stress, and the relationship between the two is inversely proportional, and the value of  $B$  is related to the characteristics of rock media, such as the brittleness, elasticity, plasticity, and fracture degree of rock.

**3.5. Moment Tensor Inversion.** Rock fracture is mainly determined by the characteristics of rock itself and the changes of surrounding rock physical conditions. The strike, type, and formation physical properties of the fault can be judged based on the dual couple component and the nondual couple component. The solution of focal mechanism is mainly realized by moment tensor inversion. There are three commonly used methods to calculate seismic moment tensor by seismic radiation mode: polarity method, amplitude method, and full waveform method. If the bias part of the moment tensor is limited, the unknown parameters can be reduced and the stability of inversion can be improved.

Moment inversion is realized by solving Green's function of elastic wave propagation. The point source propagates in a uniform elastic medium. The expressions of P-wave and S-wave amplitude are as follows:

$$A_i^P(x, t) = \frac{1}{4\pi\gamma\rho V_p^3} \gamma_i \gamma_j \gamma_k \gamma_{jk}, \quad (4)$$

$$A_i^S(x, t) = \frac{1}{4\pi\gamma\rho V_s^3} \left[ (\delta_{ij} - \gamma_i \gamma_j) \gamma_k M_{jk} \right], \quad (5)$$

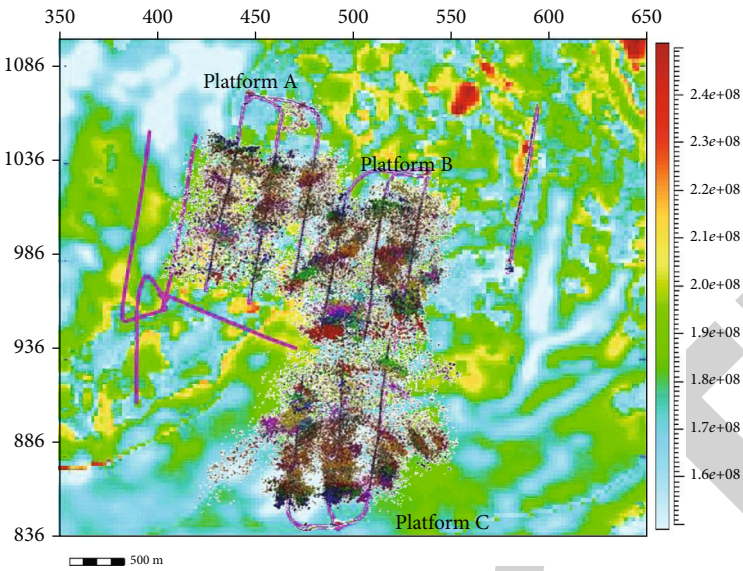
where  $VP$  and  $VS$ , respectively, represent P-wave velocity,  $X$  represents spatial position,  $T$  represents time,  $\rho$  is density, and  $R$  is the receiving distance;  $\gamma_i$ ,  $\gamma_j$ , and  $\gamma_k$  are the directions from the source to the receiver. Find cosine results, respectively;  $M_{jk}$  is the moment tensor component;  $\delta_{ij}$  is Kronecker function. Time is ignored, and the above formula is simplified:

$$u = G * m, \quad (6)$$

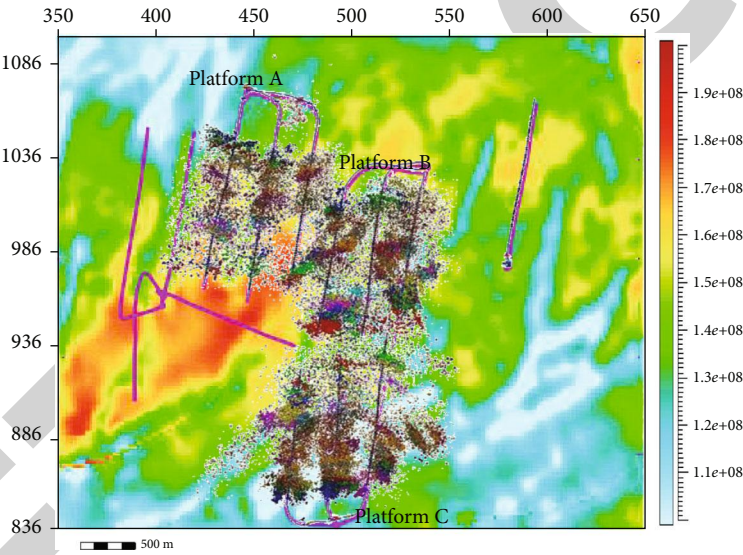
where  $u$  is displacement,  $G$  is Green matrix, and  $M$  is six independent moment tensors. Its discrete expression form is as follows:

$$\begin{bmatrix} u_1 \\ u_2 \\ \vdots \\ u_n \end{bmatrix} = \begin{bmatrix} G_{11} & G_{12} & G_{13} & G_{14} & G_{15} & G_{16} \\ G_{21} & G_{22} & G_{23} & G_{24} & G_{25} & G_{26} \\ \vdots & \vdots & \vdots & \vdots & \vdots & \vdots \\ G_{n1} & G_{n2} & G_{n3} & G_{n4} & G_{n5} & G_{n6} \end{bmatrix} \begin{bmatrix} m_1 \\ m_2 \\ \vdots \\ m_6 \end{bmatrix}. \quad (7)$$





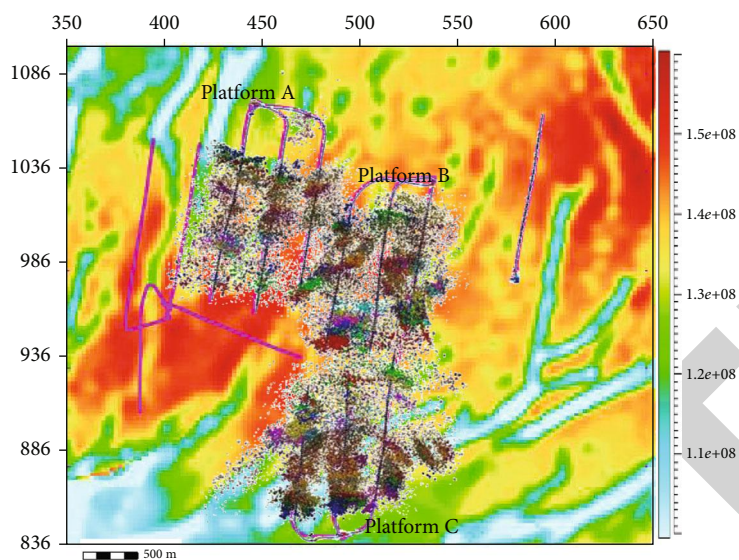
(a) Horizontal maximum principal stress



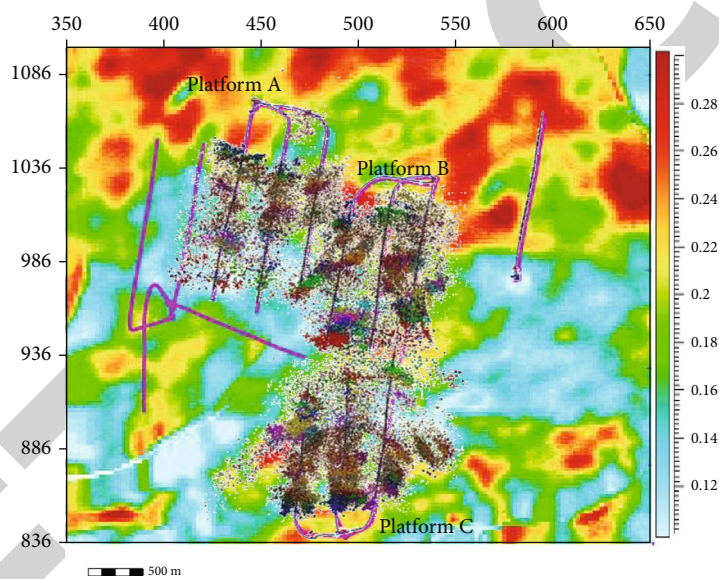
(b) Horizontal minimum principal stress

FIGURE 2: Continued.





(c) Horizontal stress difference



(d) TOC

FIGURE 2: Continued.



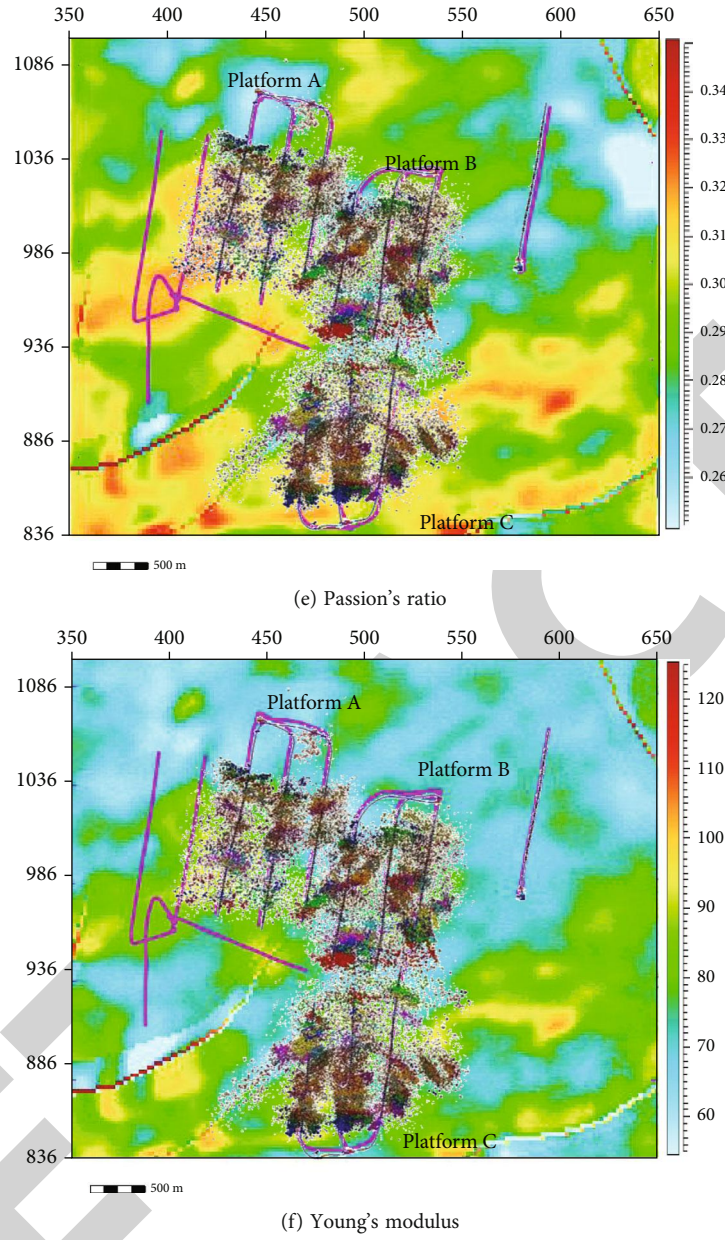


FIGURE 2: Superimposed plan of main elastic parameters and microseisms of shale gas platform in block Z in Changning area along Longmaxi Formation.

Solve the linear equations to obtain the moment tensor:

$$m = G^{-1} * d. \quad (8)$$

Because the equation is overdetermined, a large amount of data is needed to ensure the stability of the solution. Further derivation is

$$m = (G^T G)^{-1} G^T u. \quad (9)$$

Moment inversion can be realized by using seismic wave waveform, amplitude, or amplitude ratio. Sileny et al. proposed that using amplitude alone can reduce the influence

of medium uncertainty to a certain extent. Assuming that the ISO part of the volume variable is zero, the moment tensor of a single well can be solved. To complete the full moment tensor inversion, at least two monitoring wells are needed. The inversion of focal moment tensor is divided into four steps: (1) determining the spatial position of microseismic events through focal location, (2) selecting events with high signal-to-noise ratio and extracting longitudinal and transverse wave amplitudes of corresponding events, (3) calculating Green's functions corresponding to P-wave and S-wave, and (4) solve the linear equations and get six moment tensor components.

Information such as fracture direction, fracture scale, and in situ stress state can be obtained by inversion of



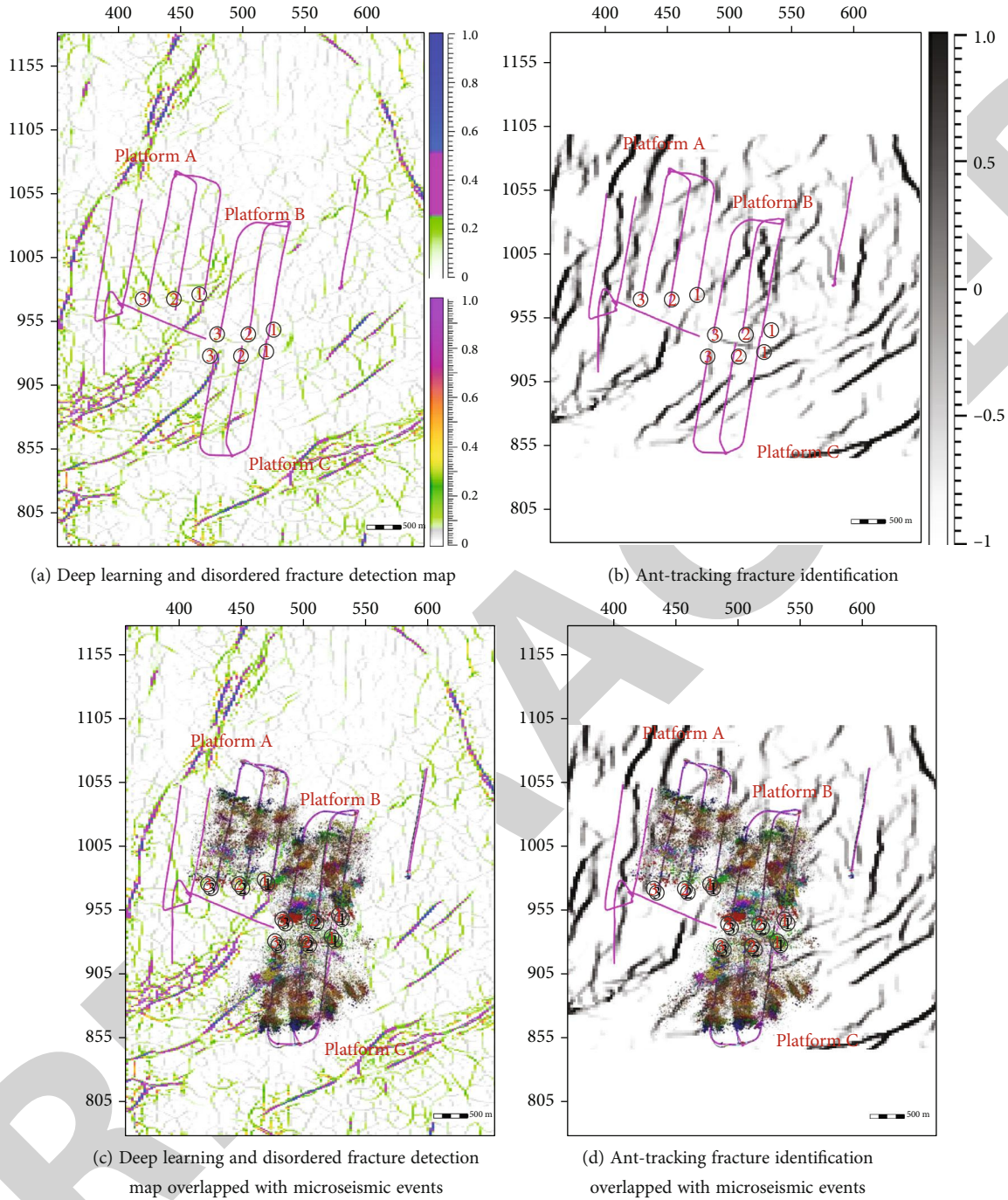


FIGURE 3: Superimposed plan of fracture prediction and microseismic events of different technologies along Longmaxi Formation of shale gas platform in block Z of Changning area.

moment tensor. Studying the solution of focal mechanism is the main way to know the characteristics of fault occurrence and rupture. It reflects the stress situation in the crust and is the basis of studying the tectonic stress field. In principle, it is necessary to use the P-wave and S-wave information of at least two wells in the way of borehole microseismic monitoring, and all the moment tensor information can be obtained through joint data inversion. If there is only one monitoring well, it is difficult to complete the inversion of moment tensor due to the lack of parameters.

#### 4. Reliability Evaluation of Microseismic Monitoring

Reliability evaluation is the basis of microseismic interpretation, which is mainly realized by analyzing microseismic signals. Evaluating the reliability of monitoring results can not only ensure the accuracy of the data used but also have a more scientific and reasonable understanding of the uncertainty in microseismic interpretation. The reliability evaluation standard is suggested to refer to three aspects:



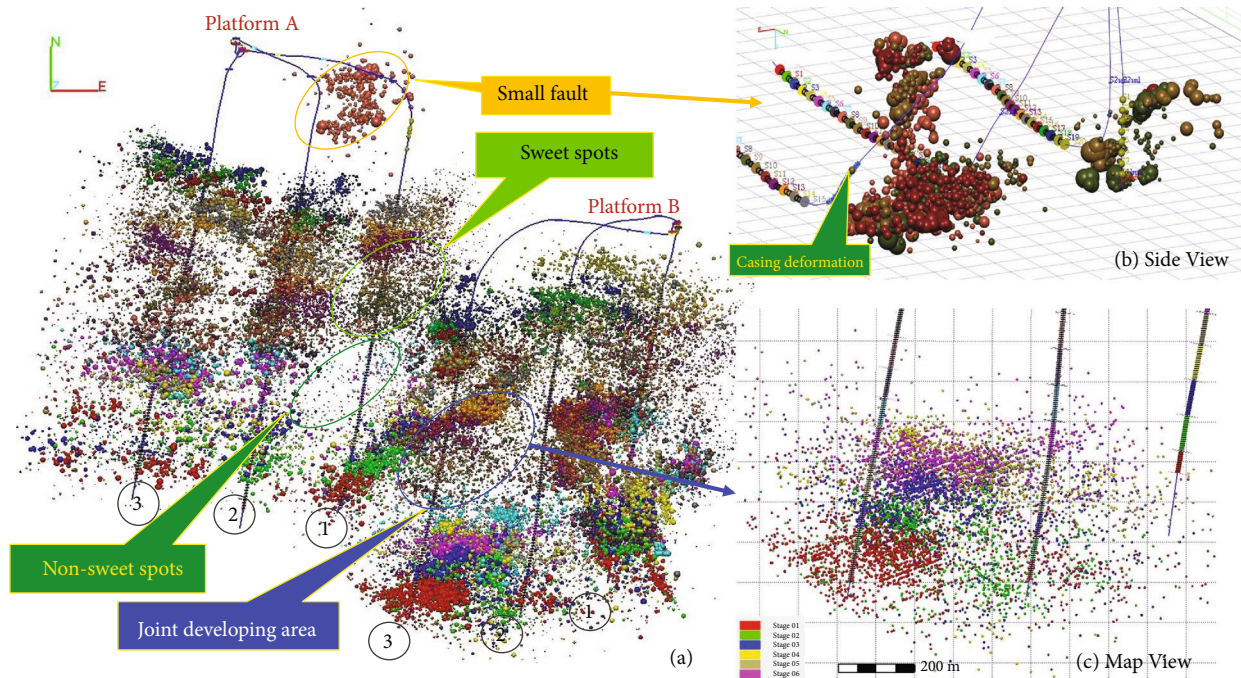


FIGURE 4: Plan of microseismic monitoring results and sample screening.

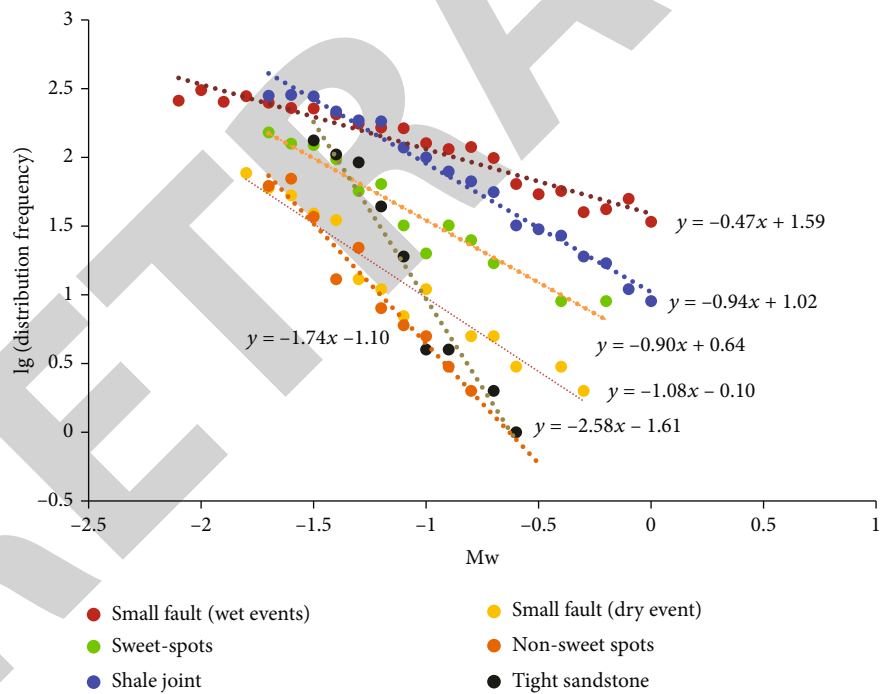


FIGURE 5: Statistics of  $B$ -values of microseismic events in different samples.

perforation or detonating cord positioning, signal-to-noise ratio, the relationship between magnitude energy, and monitoring distance.

**4.1. Perforation Positioning.** The discrimination of positioning accuracy of microseismic signal processing can only be realized if the signal position is known. Several possibilities

that can provide known positions of signals include detonating cord, perforating, and ball-throwing sliding sleeve. Because perforating or ball-throwing sliding sleeve is usually far away from geophone during the first fracturing, it is generally recommended to use detonating cord for positioning and polarization rotation of geophone before fracturing. On the premise of determining the orientation of the



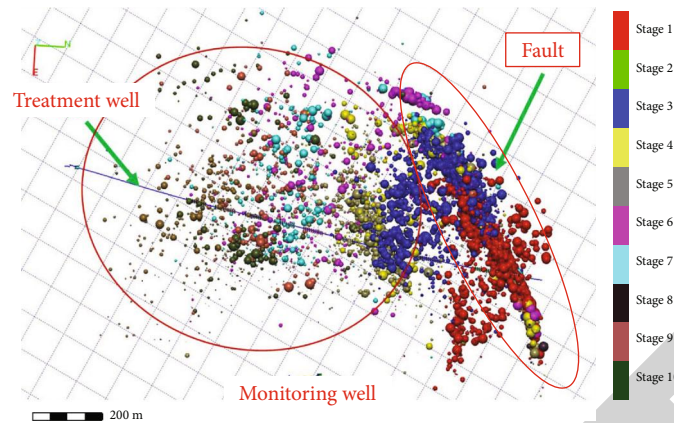


FIGURE 6: Microseismic monitoring of fault development in hydraulic fracturing of a shale gas platform in Changning.

three-component geophone, the perforation signals of each stage are located, respectively, and the corresponding positioning accuracy is statistically analyzed.

Generally, the detonating cord signal will be located close to the detector with strong energy, and the azimuth information of longitudinal wave signal is clear. As the distance between the perforation and the geophone decreases, the signal clarity increases. The positioning error of perforation is mainly caused by the uncertainty of azimuth. The overall positioning relative error (that is, the ratio of the distance between the positioning position and the perforation point to the distance between the perforation point and the geophone) is controlled within 2%, and the microseismic monitoring is reliable.

**4.2. SNR Analysis.** Signal-to-noise ratio (SNR) is another important index that needs to be paid attention to during microseismic monitoring. Using the same instrument to monitor in different monitoring wells, the signal-to-noise ratio is obviously different. Because the sensitivity of the instrument is certain, the main factor affecting the signal-to-noise ratio is the background noise. During the fracturing process, the background noise of the same monitoring well is basically stable from beginning to end, which is mainly affected by external factors such as cementing quality, geophone coupling, and well site construction. As can be seen from the intersection diagram of microseismic signal-to-noise ratio and monitoring distance in Figure 1(a), the signal-to-noise ratio of microseismic signals has nothing to do with monitoring distance, and different monitoring distances can use the same threshold value of signal-to-noise ratio to screen and identify microseismic signals.

**4.3. Analysis of Intersection between Magnitude and Monitoring Distance.** When the monitoring distance is far, the microseismic events are relatively less. Although the background noise remains unchanged with the increase of monitoring distance, the effective signal will be attenuated with the increase of propagation distance. In order to monitor signals with the same signal-to-noise ratio or higher, the farther away the microseismic events are, the higher the magnitude is. As can be seen from the intersection diagram

of moment magnitude and monitoring distance of microseismic events in Figure 1(b), the magnitude of microseismic events will increase with the increase of monitoring distance. A baseline can be obtained by referring to the minimum energy corresponding to different monitoring distances, which is mainly determined by the signal-to-noise ratio, and the threshold value of signal-to-noise ratio of the same monitoring well is determined.

From the intersection of moment magnitude and signal-to-noise ratio of microseismic events (Figure 1(c)), it can be seen that there is a certain linear relationship between them, and the signal-to-noise ratio of microseismic signals will increase with the increase of magnitude. Because the background noise is relatively stable, the higher the effective signal energy, the higher the natural signal-to-noise ratio will be.

Through the above analysis on the relationship between perforation signal, micro seismic signal signal to noise ratio, magnitude and monitoring distance. On the one hand, we can judge the reliability of microseismic interpretation data sources (microseismic processing results) and combine the understanding of possible precision problems in microseismic processing to better serve microseismic interpretation. On the other hand, the different threshold values of signal-to-noise ratio of microseismic signals received by different monitoring wells in the same instrument show that improving signal-to-noise ratio is the key to reduce errors and improve signal reliability.

## 5. Evaluation of Fracturing Effect

The accuracy of microseismic fault identification is much higher than that of seismic identification technology, which is mainly due to the problems existing in earthquake prediction and the advantages of microseismic fault identification. Even if the seismic acquisition conditions are good and the processing process is accurate, the processed seismic data itself has inherent limitations such as signal-to-noise ratio and resolution, and the response of seismic data to small faults and fractures is very weak or no response, especially for microfractures, which is very difficult to predict and



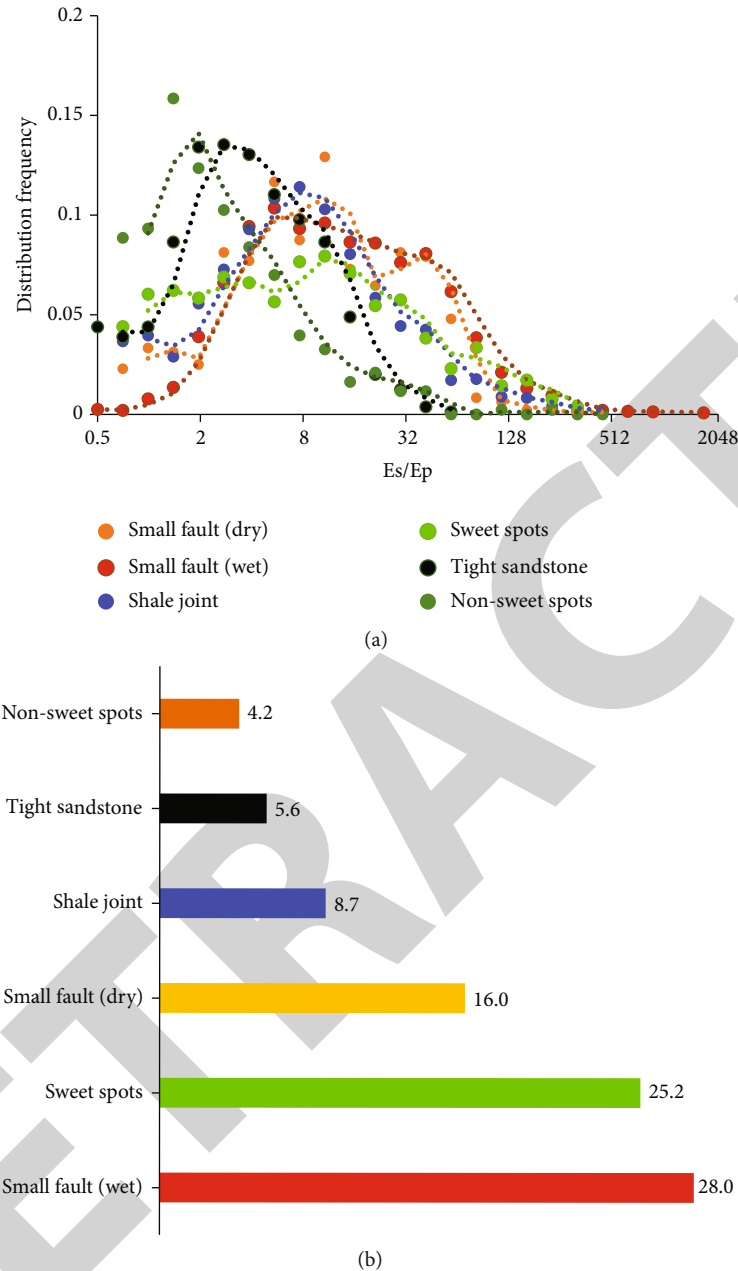


FIGURE 7: Probability statistics of  $Es/Ep$  value distribution and  $Es/Ep$  mean statistics of different microseismic event samples.

has certain multisolutions. However, microseismic monitoring (taking underground monitoring as an example) locates the fracture response caused by fracturing by placing the instrument in the well and collecting the direct wave. The interference of this monitoring method is far less than that of the surface acquisition, and because the direct wave is collected, the monitoring distance is closer than that of the surface acquisition, and the signal reliability is higher. On the other hand, from the response mode, compared with the interface reflection wave transmitted to the surface through the static fracture, microseismic monitoring can easily identify the fracture by receiving the signal generated by the dynamic stretching or shearing of the fracture through the geophone. Microseismic monitoring can not only identify

microcracks, joints, and faults but also monitor a large number of artificial joints.

When there is inconsistency between the results of earthquake and microseismic, on the premise of qualified microseismic quality control, processing, and other analysis work, the microseismic results should be recognized as more reliable at first, and then, the fracture evaluation work combining microseismic and multidisciplinary can be carried out.

#### 5.1. Verification of Evaluation Results of Reservoir Elements.

Taking the microseismic fracturing monitoring of three Longmaxi shale gas platforms A, B, and C in a block in Changning area as an example, the relationship between well trajectory and structural strike is as follows: platform A



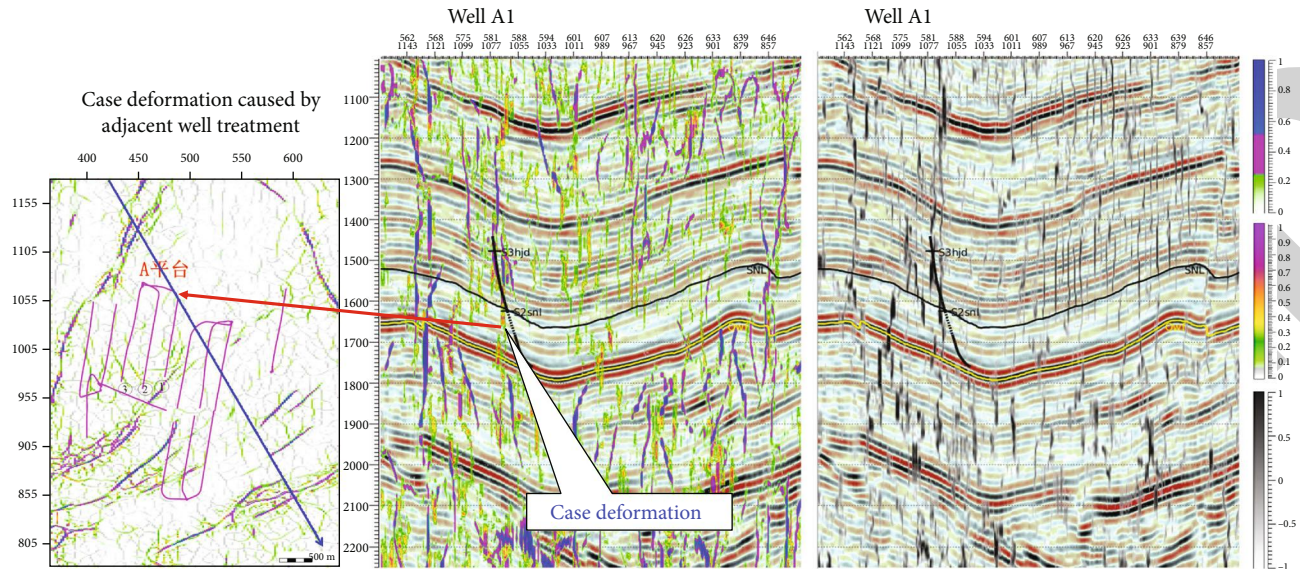


FIGURE 8: Cross-section of seismic multiscale fracture detection and ant body fracture identification in well 1 of platform A.

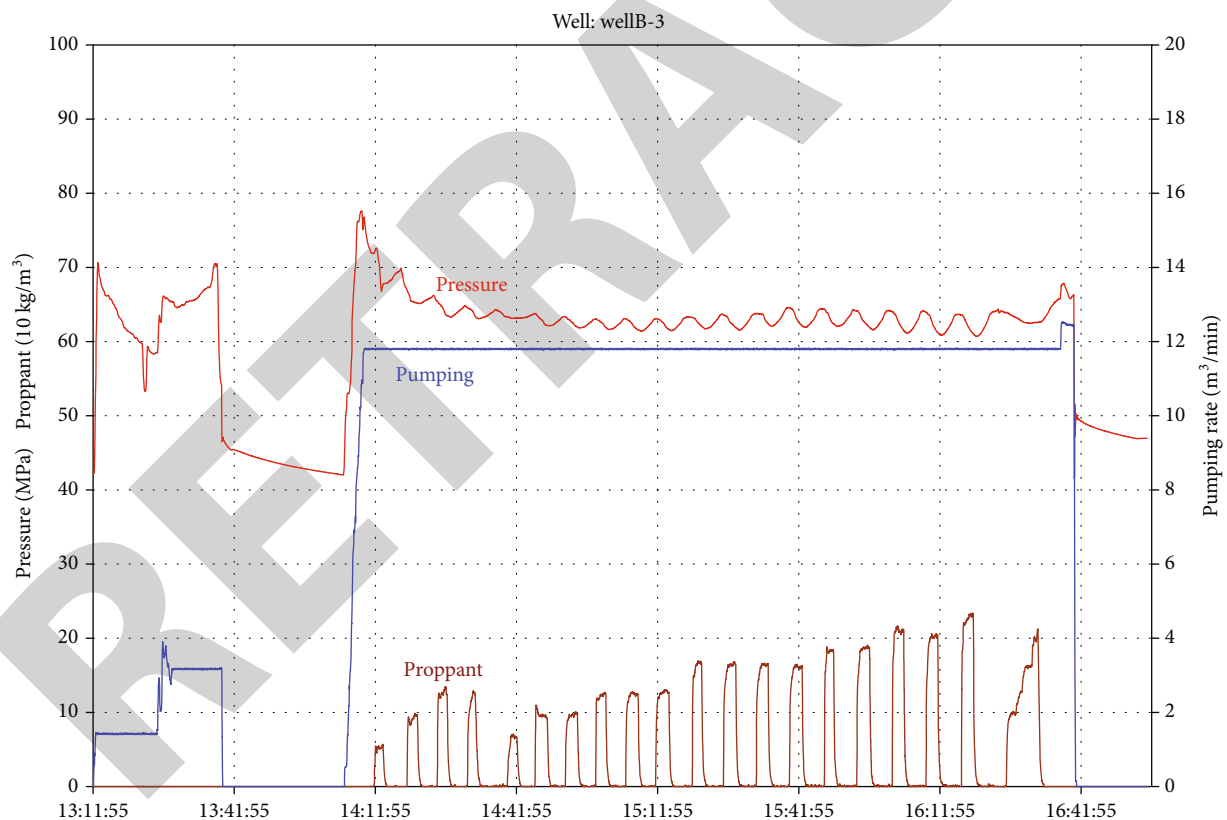


FIGURE 9: Fracturing construction curve under microseismic monitoring of shale joint development.

inclines from north to south, platform B rises from north to south, and platform C inclines from south to north. The horizon is the bottom of Wufeng Formation, and none of the three wells drilled through the lower carbonate formation.

Based on the seismic data, the geological-engineering double desert prediction of the three platforms is com-

pleted, and a series of elastic parameters (horizontal maximum principal stress, horizontal minimum principal stress, horizontal maximum and minimum stress difference, TOC, Young's modulus, and Poisson's ratio) which can reflect the characteristics of the matrix are obtained, as well as multiscale fracture detection bodies and ant bodies, etc. The plane attributes of elastic parameters are extracted along



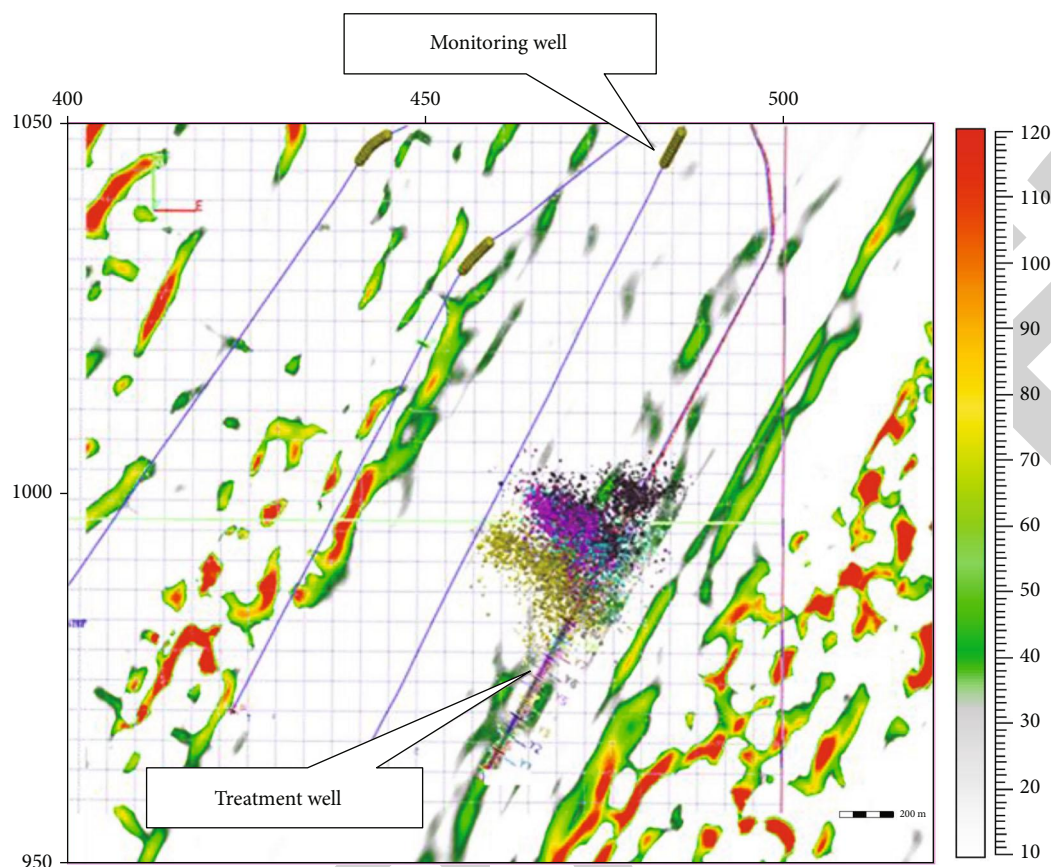


FIGURE 10: Superposition of microseismic monitoring and curvature prediction.

the bottom of Longmaxi, respectively, and the plane diagram of elastic parameters is obtained (Figure 2). It can be seen from the figure that the favorable sweet spot area is characterized by four lows and two highs on the elastic parameters, namely, low maximum horizontal principal stress, minimum horizontal principal stress, horizontal maximum minimum stress difference, Poisson's ratio, high TOC, and Young's modulus. On the whole, except for the high in situ stress in the first half of platform A, most of the other positions show "sweet spot" characteristics. The superposition of elastic parameters and microseismic data further confirms the development characteristics of this fracturing fracture. Among the three platforms, the overall geostress of platform A is the highest, followed by platform B and platform C, which is consistent with the highest pressure of well A and the lowest pressure of well C in the fracturing process. Moreover, the microseismic events monitored by platform C are the most, followed by platform B, and platform A is the least.

Multiscale fracture detection technology combining deep learning with messy detection is used for fracture prediction, and the fracture detection plan of Longmaxi Formation is obtained (Figure 3). From the prediction results, the multiscale prediction results are hierarchical, and it is easy to distinguish faults from fractures. Except that there are two small faults near the toe of well A and well C on platform C, there are no faults drilled on the whole. The cracks predicted by ants are relatively developed. The superposition

of fracture prediction results and microseismic results shows that there is a very good correspondence on the whole. For example, the microseismic events near the small fracture of platform A have strong energy (the size of the event points represents the intensity), and the characteristics of extending along the northeast of the fracture are obvious. During the first few fracturing stages of well C on platform C, microseismic events continue to extend to the southwest of the fracture, indicating that the two small fault zones are very consistent with the actual microseismic results. The response of ants to cracks is also a good reference. For example, the cracks in the first half of platform B that extend from northeast to the second half of platform B turn to north-south, and the distribution characteristics of strong and microseismic events are also consistent with them. The NE-trending fractures in the second half of platform C are similar to the NE-trending microseismic events. Judging from the trend and development characteristics of fractures, the well trajectory can be appropriately shifted from the north to the east, and the fracturing effect will be better.

**5.2. Fracture Identification and Evaluation.** When the earthquake prediction results are inconsistent with the microseismic monitoring results, and unexpected conditions occur during fracturing, it is necessary to check the earthquake data, especially to see if there is any omission in the fracture prediction or the earthquake prediction results are inaccurate. In the



process of fracturing, when fracturing fluid enters fault, natural fracture, joint development area, page dessert area, nondessert area, and other areas, microseismic data show different manifestations. However, at present, the understanding of the initiation and propagation laws of shale fracturing fractures is not perfect. It is necessary to carry out further research on the initiation and propagation laws and characterization of complex fracture networks, clarify the fracture network structure of volume fracturing, and provide a reasonable and accurate basis for the formulation of field construction parameters and construction effect evaluation of shale gas development strategies. Based on this, this paper proposes a process of fracture identification and evaluation that combines microseismic data mining with multidisciplinary information (earthquake, geology, drilling, fracturing, etc.).

Figure 4 shows the top view of microseismic monitoring results of platform A and platform B, in which each fracturing stage is represented by a separate color, and the moment magnitude is represented by the magnitude of the event. Data representing different characteristic areas are selected as samples to analyze microseismic signals, including small faults, joint development areas, dessert areas (most areas are dessert areas), and nondessert areas. Among them, the microseismic events in the small faults have obvious longitudinal span, and the crisscross microseismic signals are also detected in the joint area (displayed in equal size of events), and the events in the nondessert area are relatively few and the energy is weak.

According to the  $B$ -value statistics of the sampled data (Figure 5), it is found that the  $B$ -value of shale joint area is  $-0.94$ , that of minor faults is  $-1.08$ , that of most shale dessert areas is around  $-0.9$ , and that of nondessert areas is  $-1.74$ , with obvious differences. Because the fault of this platform is passively activated (caused by dry events without fracturing fluid entering the fault), it cannot completely reflect the  $B$ -value characteristics of fracturing fluid entering the fault. In order to better reflect the difference of  $B$ -values under different stratum characteristics, the data sample of another platform fault in the adjacent area (Figure 6) is introduced to calculate the  $B$ -value as  $-0.47$ . It can be seen that when fracturing fluid enters the fault-activated fault, the  $B$ -value of microseismic events obtained is the highest, and the black event point is a tight one in the east. To sum up, it can be seen that faults (dry events and wet events), cracks, dessert development areas, and nondessert development areas can be well distinguished by  $B$ -value statistics.

Because the shear wave energy intensity is determined by the medium rigidity coefficient, dislocation amount, and fracture surface area, the energy of faults, fractures, and dense sections will be different. Compared with fracture areas, the joint area is different in that it generally presents the characteristics of X-shaped conjugation, and tensile fractures and shear fractures exist simultaneously during fracturing. According to the  $E_s/E_p$  energy statistics of the above-mentioned different areas (Figure 7(a)), it can be seen that the peak interval of  $E_s/E_p$  range of fault response of the highest dry event is similar to that of wet event, the peak interval of shale joint and dessert area is smaller than that of fault, the peak interval of tight sandstone layer is smaller

than that of joint and dessert area, and the peak interval of shale nondessert area is the lowest. Further calculate the  $E_s/E_p$  mean statistics of the above data points (Figure 7(b)), and the order is as follows: small fault (wet event) > shale sweet spot area > small fault (dry event) > shale joints > tight sandstone layer > shale nonsweet spot area.

The existence of faults is easy to cause construction accidents or risks. During the fracturing of well A on platform A, an accident happened because of the existence of faults. When fracturing the second stage of well 1 on platform A, there was always a sticking problem in the process of setting the perforating gun, which could not be set down. During the first-stage fracturing of wells A and B, not only a large number of microseismic signals were received near the perforating section, but also a large number of strong-energy microseismic signals near the deflecting section were monitored. After picking up and locating these signals in the later period, a large number of microseismic events are obtained. From the shape and magnitude, it is preliminarily judged that there may be faults, and casing deformation is caused by strata dislocation caused by hydraulic fracturing (Figure 4(b)). Combined with  $B$ -value statistics and  $E_s/E_p$  statistics, the existence of faults is further verified.

Combined with the prediction results of seismic data in this area (Figure 8), the development of faults near the kick-off section of well A on platform A was found on multi-scale fault detection bodies and ant bodies, respectively. Although the fault characteristics on the seismic profile near the kick-off section are not particularly obvious, the predicted faults above and below this section are also very obvious, and the faults are relatively reliable.

If it is simply fracturing of three horizontal wells on this platform, the perforation section is far from the kick-off section at the beginning of fracturing, so it will not generate such strong energy in the kick-off section. After investigation in the nearby well site, it is found that the northern platform which is really adjacent to this platform is undergoing fracturing construction. As this platform does not belong to the scope of mining rights of this oilfield, after providing the demonstration of microseismic monitoring results, it is agreed with the other party to suspend the related operations of this platform through consultation and then continue after the fracturing of this well is finished. Because the fault exists, the reason why the perforating gun cannot be lowered is found, that is, the casing deformation caused by the fault. From the engineering point of view, the solution was found, and finally, the coiled tubing sandblasting perforation method was adopted, and finally, it was successful.

It can also be seen from this example that before the fracturing operation monitoring starts, it is necessary to have a comprehensive understanding of the geological conditions in this area. If necessary, it is necessary to suspend drilling and fracturing operations in the adjacent area, so as to prevent signal interference on the one hand and influence on construction on the other.

It is ideal that shale joints exist in the fracturing process. Under this stratum condition, the stratum is brittle, and the communication of microcracks between shale joints is also



conductive to the preservation of shale gas. Figure 4(c) shows the fracturing monitoring effect of platform B. It can be seen that there are obvious parallel joint structures developed between the two wells, and the main direction is 70 degrees northeast. The average spacing between joints is 15 m, and the minimum spacing is about 10 m. In the range of  $400 \times 400$  m between the two wells, there are about 30 conjugate joints, with the longest length of about 670 m.

During the monitoring of hydraulic fracturing on this platform, due to the existence of conjugate joints, the pump pressure will rise in stages (Figure 9). The main reason is that when the fracturing fluid advances rapidly along the joint direction, the fracturing fluid will have certain filtration failure. When the fracturing fluid enters the joint corner, there will be a certain pressure hold-up. When this position is flushed away, the fracturing fluid will move forward quickly, and when it meets the next corner, it will hold back pressure again, so the pressure curve will change from high to low. From the statistics of microseismic event  $B$ -value and  $E_s/E_p$ , it can be seen that the shale sweet spot area is similar to the joint area  $B$ -value, but the joint area  $E_s/E_p$  value is slightly smaller than the sweet spot area, indicating that the opening of a series of joints makes the  $E_s/E_p$  value lower when the pressure rises.

**5.3. Fracturing Barrier.** The existence of natural fractures will also form a fracturing barrier. The so-called fracture barrier refers to the natural fractures or faults that the fractures produced by hydraulic fracturing cannot penetrate and prevent the hydraulic fractures from extending. This concept was first put forward by Maxwell (2016). Or fault fractures can be divided into open fractures and closed fractures. The extension direction of the fracture corresponding to the open fracture is the same as the extension direction of the maximum principal stress of the regional stratum. This fracture has conductivity and can provide a flow channel for fracturing fluid. The extension direction of the fault or fracture corresponding to the closed fracture is perpendicular to the direction of the maximum principal stress in the region or obliquely crosses at a large angle, and the fault or fracture plays a blocking role, forming a fracturing barrier. When the fracture generated by hydraulic fracturing extends here, it will stop extending, and the fracturing energy will be released to both sides along the fracture, even forming sand plugging. Curvature reflects the structural form of strata. Nelson shows that there is a good positive correlation between the maximum curvature value and the maximum strain value in rocks, so the fracture can be predicted by curvature attribute. Usually, the natural fracture development zone is characterized by high curvature. When the development direction of natural cracks is perpendicular to the current stress direction, they are subjected to stress to form closed cracks.

Figure 10 shows the fracturing monitoring results of a shale gas horizontal well in Fuling block, with a grid interval of  $100 \times 100$  m, and the microseisms are expressed in the form of event points with the maximum curvature attribute in the background. It can be seen from the figure that most of the microseismic events are distributed in the west side

of the wellbore, and they can extend as far as the west side of the horizontal well, with an extension distance of nearly 400 m. The east crack stops developing after a short extension. Fractured fractures in the 14th and 15th sections extend in the east and west sides, and the west side extends normally, but they are affected by the fracturing barrier on the east side of the wellbore. After reaching the fracturing barrier, the fractures extend along the fracturing barrier to the northeast. According to the comprehensive geological evaluation study, the current horizontal maximum principal stress direction is NW-SW, so the cracks on the curved body on the east side of the wellbore are closed cracks, which play the role of fracturing barrier.

## 6. Conclusion

The comprehensive evaluation of microseisms is realized by comprehensive analysis of source signals. In this paper, the source information of microseisms is systematically divided. Five methods of seismic source information analysis are summarized and put forward. Principle and idea of advocating reliability evaluation first for fracturing evaluation. According to the fracturing effect evaluation, the comprehensive evaluation technology and ideas of multidisciplinary matrix integration and fracture and engineering integration are put forward, and the following results are obtained:

- (1) That source information is a series of information obtained by direct or indirect calculation in the process of microseismic monitoring. In this paper, the information is systematically divided and explain, including microseismic signal type, time, position information, precision parameters, source-related parameters, focal mechanism-related parameters, and quality control-related parameters
- (2) Seismic source information analysis is the basis of microseismic evaluation. This paper puts forward and explains the research methods of microseismic signal analysis from five aspects: statistical analysis, intersection analysis, fracture surface and nodal surface, magnitude-frequency gradient  $B$ -value analysis, and moment tensor inversion
- (3) Reliability evaluation of microseismic signal is the basis of microseismic interpretation. This paper puts forward three criteria for reliability evaluation: perforation or detonating cord positioning, signal-to-noise ratio, and the intersection relationship between magnitude energy and monitoring distance. On the premise of ensuring the accuracy of adopted data, reliability evaluation can make a more scientific and reasonable judgment on the uncertainty in microseismic interpretation
- (4) A multidisciplinary integrated microseismic comprehensive interpretation technology is put forward, which combines microseismic with engineering construction such as drilling and fracturing with geological, seismic, and logging evaluation. The



multidisciplinary fracturing evaluation technology is established from three aspects: verification of reservoir element evaluation results, identification and evaluation of fractures, and interpretation of fracturing barriers

## Data Availability

The figures and tables used to support the findings of this study are included in the article.

## Conflicts of Interest

The authors declare that they have no conflicts of interest.

## Acknowledgments

The authors would like to show sincere thanks to the contributors of the techniques used in this research.

## References

- [1] C. D. Jenkins and C. M. Bayer, "Coalbed- and shale-gas reservoirs," *Journal of Petroleum Technology*, vol. 60, no. 2, pp. 92–99, 2008.
- [2] E. Ozkan, "The way ahead for US unconventional reservoirs," *The Way Ahead*, vol. 10, no. 3, pp. 37–39, 2014.
- [3] E. M. Scordilis, "Empirical global relations converting MS and Mb to moment magnitude," *Journal of Seismology*, vol. 10, no. 2, pp. 225–236, 2006.
- [4] T. C. Hanks and H. Kanamori, "A moment magnitude scale," *Journal of Geophysical Research: Solid Earth*, vol. 84, no. B5, pp. 2348–2350, 1979.
- [5] H. Kanamori, "The energy release in great earthquakes," *Journal of Geophysical Research*, vol. 82, no. 20, pp. 2981–2987, 1977.
- [6] G. Purcaru and H. Berckhemer, "A magnitude scale for very large earthquakes," *Tectonophysics*, vol. 49, no. 3–4, pp. 189–198, 1978.
- [7] G. Purcaru and H. Berckhemer, "Quantitative relations of seismic source parameters and a classification of earthquakes," *Tectonophysics*, vol. 84, no. 1, pp. 57–128, 1982.
- [8] C. Yuntai and L. Ruifeng, "Moment magnitude and its calculation," *Seismological and Geomagnetic Observation and Research*, vol. 39, no. 2, pp. 1–9, 2018.
- [9] H. Cheng, Y. Dong, C. Lu, Q. Qin, and D. Cadasse, "Intelligent oil production stratified water injection technology," *Wireless Communications and Mobile Computing*, vol. 2022, Article ID 3954446, 7 pages, 2022.
- [10] J. T. Rutledge and W. S. Phillips, "Hydraulic stimulation of natural fractures as revealed by induced microearthquakes, Carthage Cotton Valley gas field, east Texas," *Geophysics*, vol. 68, no. 2, pp. 441–452, 2003.
- [11] Z. K. Hou, H. L. Cheng, S. W. Sun, J. Chen, D. Q. Qi, and Z. B. Liu, "Crack propagation and hydraulic fracturing in different lithologies," *Applied Geophysics*, vol. 16, no. 2, pp. 243–251, 2019.
- [12] B. Gutenberg and C. F. Richter, "Earthquake magnitude, intensity, energy, and acceleration," *Bulletin of the Seismological Society of America*, vol. 46, no. 2, pp. 105–145, 1956.
- [13] J. Sileny, G. F. Panza, and P. Campus, "Waveform inversion for point source moment tensor retrieval with variable hypocentral depth and structural model," *Geophysical Journal International*, vol. 109, no. 2, pp. 259–274, 1992.
- [14] J. Sileny and A. Milev, "Source mechanism of mining induced seismic events – resolution of double couple and non double couple models," *Tectonophysics*, vol. 456, no. 1–2, pp. 3–15, 2008.
- [15] J. Han, H. Cheng, Y. Shi, L. Wang, Y. Song, and W. Zhnag, "Connectivity analysis and application of fracture cave carbonate reservoir in Tazhong," *Science Technology and Engineering*, vol. 16, no. 5, pp. 147–152, 2016.
- [16] Z. Jechumtálová and J. Šílený, "Amplitude ratios for complete moment tensor retrieval," *Geophysical Research Letters*, vol. 32, no. 22, pp. 1–5, 2005.
- [17] H. Cheng, P. Ma, G. Dong, S. Zhang, J. Wei, and Q. Qin, "Characteristics of carboniferous volcanic reservoirs in Beisantai Oilfield, Junggar Basin," *Mathematical Problems in Engineering*, vol. 2022, Article ID 7800630, 10 pages, 2022.
- [18] V. Vavryčuk, "On the retrieval of moment tensors from borehole data," *Geophysical Prospecting*, vol. 55, no. 3, pp. 381–391, 2007.
- [19] H. Cheng, J. Wei, and Z. Cheng, "Study on sedimentary facies and reservoir characteristics of Paleogene sandstone in Yingmaili block, Tarim Basin," *Geofluids*, vol. 2022, Article ID 1445395, 14 pages, 2022.
- [20] L. Han and Y. Zhenxing, "Solving the focal mechanism of microseisms based on the frequency domain of "shear+tensile fracture" general dislocation model," *Journal of Geophysics*, vol. 61, no. 3, pp. 905–916, 2018.